

## NUMERICAL SIMULATION OF TURBULENT DISPERSION ON A TWO-WAY FACING TRAFFIC ROAD

Ryusuke Yasuda<sup>1</sup>, Takeyuki Miyajima<sup>1</sup> and Atsumasa Yoshida<sup>1</sup>

<sup>1</sup>Osaka Prefecture University, Osaka, Japan

### INTRODUCTION

Air pollution around heavy traffic road is one of major urban problems in Japan. For seriously polluted areas, modification of the road structure and/or application of some kind of air purification system that sucks polluted air within the roadway are planned to suppress the high concentration levels. Reynolds-Averaged Navier-Stokes (RANS) model is often used to predict such micro-scale air quality, however, the treatment of the vehicle-induced turbulence is ambiguous. To establish appropriate methodology for such RANS simulations, it is necessary to know the details of the turbulent dispersion process of the vehicle exhausts within the roadway.

In this study, we conducted a series of numerical experiments to investigate vehicle-induced turbulence and its effect on the turbulent dispersion within a one-way and a two-way traffic road. A Large Eddy Simulation (LES) model was developed to reproduce the instantaneous behaviour of the exhaust gas emitted from running vehicles. To represent the movement of each vehicle by numerical grids explicitly, we used a sliding mesh method. The configuration of the road is straight, infinite length and flat. Results of the one-way traffic case were compared with those of the two-way facing traffic case. Note that the influences of heat and the rotation of tires are not considered in this study.

### NUMERICAL METHOD AND CALCULATION CONDITIONS

LES technique was used to reproduce unsteady, three-dimensional turbulent flow. The conservation equations of mass, momentum and passive scalar were discretized by a finite volume method on a staggered grid system. For the momentum equation, the second-order Adams-Bashforth scheme was used for the time derivatives and QUICK scheme was employed for the advection terms. For the advection terms in the scalar conservation equation, Walcek's scheme (Walcek, 2002) was used to prevent the occurrence of negative concentration. A second-order central difference scheme was applied for all other special derivatives. The sub-grid scale (SGS) turbulent viscosity was estimated by using Smagorinsky model and the SGS turbulent diffusion coefficient was given by the SGS turbulent viscosity and a turbulent Schmidt number. SMAC method was used for the velocity-pressure coupling. For the two-way facing traffic case, a sliding mesh method was used to express the relative movement between the vehicles and the ground surface (Fig.1).

The calculation condition is summarized in Table 1. A non-uniform grid system was used to increase resolution near the vehicles and the ground surface. The x-axis is parallel to the roadway, the y-axis is perpendicular to it and z-axis is vertical. All vehicles were assumed to be a sedan type and moving at 40 km h<sup>-1</sup> (=11.1 m s<sup>-1</sup>;  $U_c$ ) with 3 s intervals. A tail pipe with 0.07 m diameter was located at the rear end of the vehicle on the right hand side from the driver's view. Exhaust gas was emitted at 3.2 m s<sup>-1</sup> from it. A periodic condition was imposed on the x boundaries to represent the successive passing of vehicles by a finite number of grids. Two-layer model (Werner *et al.*, 1999) was applied on the solid surface boundaries. The origin of the coordinate system ( $y=z=0$ ) is at the outer edge of the vehicle body and on the ground surface. The origin of the x-axis is at the rear edge of the vehicle from the vehicle-

fixed frame. Note that there is no particular position in the  $x$ -direction from the road-fixed frame.

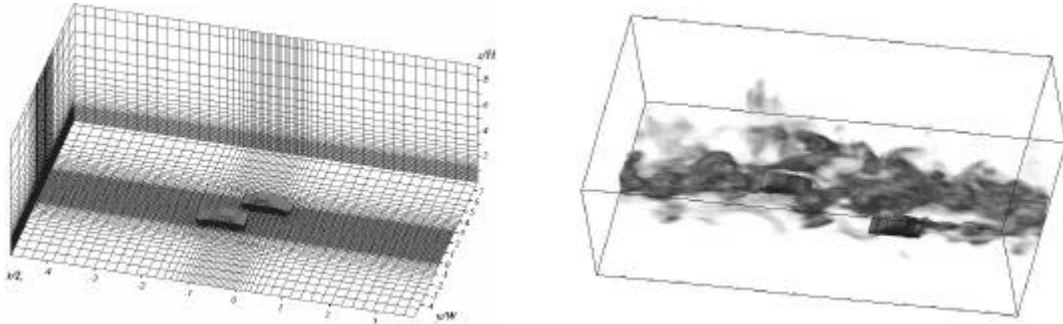


Fig.1; The grid configuration and a snapshot of concentration distribution.

Table 1. Calculation conditions

Cases	One-way (A0, A1, A2)	Two-way (B0, B1,B2)
Domain size ( $x,y,z$ ) (m)	(37.6,16.7,12.9)	(37.6, 21.6,12.9)
Grid number	(119, 95, 62)	(119,148,62)
Vehicle size ( $L,W,H$ ) (m)	(4.38,1.70,1.46)	
Grid number	(36,25,23)	
Grid interval (m)	$D_x=0.12\sim0.48$ , $D_y=0.07\sim0.68$ , $D_z=0.05\sim1.07$	
Tail pipe position ( $y/W, z/H$ )	(0.92,0.15)	(0.92,0.15), (2.00,0.15)
Time step	$\Delta t=0.004 T^*$ , $T^*=W/U_c$	
Reynolds number	$Re=1.20\times 10^6$	
Turbulent Schmidt number	$Sc_t=0.5$	

To investigate the influence of cross flow on the turbulent dispersion of the exhaust gas, a background approaching flow, which is perpendicular to the roadway and has 1/4 power profile, was given. The reference velocity of the approaching flow,  $V_a$ , is defined at 10 m above the ground surface. The first index of each run-case designates one-way (A) or two-way facing (B) traffic, and the second index (0,1,2) shows the speed of the approaching flow ( $V_a=0, 1.0, 2.0 \text{ m s}^{-1}$ ) respectively. For the approaching flow, no perturbation velocity was imposed. Concentration calculation was executed only in the case of cross flow existing.

## RESULTS AND DISCUSSION

Since the calculation conditions of the flow and the concentration fields are uniform in the  $x$  direction from the view of the road-fixed frame, the instantaneous variables were averaged not only in time but also in  $x$  direction to obtain the distributions of the mean statistics on the cross section normal to the roadway. After the flow field reached a statistically steady state, the instantaneous flow variables were averaged in time and space. The averaging period is  $240T^*$ , which corresponds to the period of 12 vehicles passing. For concentration field, the mean statistics were estimated during the last  $120T^*$ . Within the vehicle's grid,  $(u,v,w)=(U_c,0,0)$  and  $c=0$ , where  $(u,v,w)$  are instantaneous velocity components in  $x,y,z$  direction and  $c$  is instantaneous concentration. All concentration values were non-dimensionalized by  $c^*=cV_aW^2/Q$ , where  $Q$  is the emission rate. Because the contribution of the SGS components are very small compared to the Grid-scale (GS) components except in the vicinity of the solid surface, the SGS contribution are not included for all second moment statistics. Hereafter, we call the projection area of passing vehicles on  $y-z$  plane as a "passing area".

Fig.2 shows the mean velocity vector on the y-z cross section in calm condition. In the one-way traffic case (Case-A0), a pair of trailing vortices is clearly observed and downdraft exists in and over the passing area. Near the ground surface, the downdraft changes its direction to the spanwise and flows out from the passing area. In the two-way facing traffic case (Case-B0), in addition to the downdraft over each lane, updraft is also observed on the region between the two lanes, which is caused by a impingement of the spanwise flow from the vehicles on each lane. Though the mean flow pattern is significantly different between these two cases, the influence on the pollutant dispersion will not be so strong except in calm condition because the magnitude of the mean flow is relatively small (less than  $0.05U_c$ ).

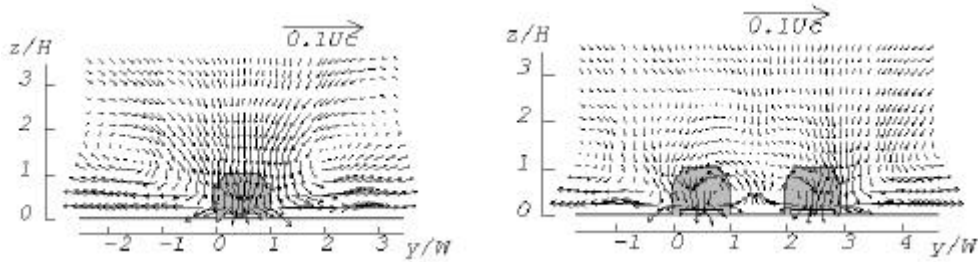


Fig.2; Mean velocity vector on the y-z cross section. (left:Case-A0,right:Case-B0).

The turbulence kinetic energy ( $k$ ) in the passing area shows a high value and distributes almost uniformly in it. The maximum value of  $k$  is  $0.04 U_c^2$  in Case-A0, and  $0.05 U_c^2$  in Case-B0. In both cases, the  $k$  decreases rapidly outside of the passing area; it reduces to  $0.002U_c^2$  at one  $W$  away from the area. Fig.3 shows the spanwise profiles of the turbulence intensities ( $s_v/\sqrt{U_c}, s_w/\sqrt{U_c}$ ) in Case-A0,B0, where  $s_v$  and  $s_w$  are the standard deviation of the spanwise and the vertical velocities, respectively. The vertical levels of these profiles ( $z/H=0.05$  and  $0.50$ ) are chosen as the height where their maximum values are observed. The maximum value of the  $s_v$  appears at the outer-bottom edge of the passing area. In the two-way traffic case, the magnitude of  $s_v$  near the centreline is intensified by the vehicles running on the opposite lane. The position where the maximum  $s_w$  appears is near the mid-point of the passing area in this cases, but it would depend on the shape of vehicles. The maximum values of the turbulence intensities in Case-A0 and B0 are not so much different and their order is about  $0.1U_c$ . Because such values of fluctuation velocity ( $s_v, s_w \sim 1 \text{ m s}^{-1}$ ) are comparable to the fluctuation observed when the mean wind is  $5 \sim 10 \text{ m s}^{-1}$ , the influence of the vehicle-induced turbulence on pollutant dispersion on the roadway is important.

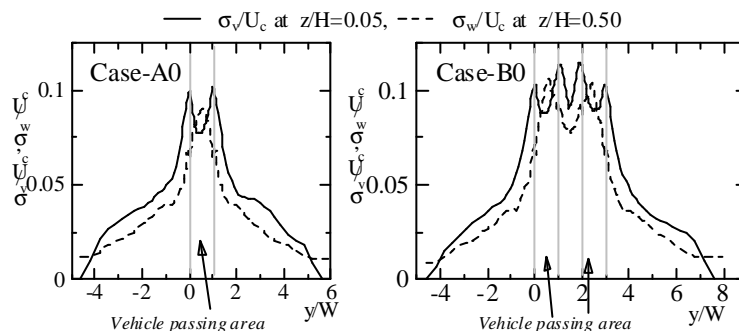


Fig.3; Spanwise profiles of turbulence intensities.

Fig.4 shows the distributions of the time-space averaged velocity vector on the y-z cross section. When cross flow perpendicular to the roadway exists, vehicle circumventing flow is superimposed on the cross flow. In the one-way traffic case (Case-A1,A2), only one vortex is observed within the passing area, in contrast to the calm case (Case-A0) in which there is a

pair of vortices outside of the area. In the two-way facing traffic case, a pair of vortices is observed near the centreline side of the each passing area in calm condition (Case-B0), on the other hand, the centre of the vortices move to the upwind side within the each passing area when the cross flow exists (Case-B1,B2). When cross flow exists, the magnitude of  $s_v$  and  $s_w$  are remarkably reduced in the upwind side of the passing area and slightly increased in the lee side of it in comparison with the case of calm condition. Though the magnitude of  $s_v$  and  $s_w$  within the passing area also slightly increase according to the increase of the cross flow velocity, the maximum value does not increase and shows a value of  $0.1U_c$  approximately.

In Fig.4 also shows the distributions of mean concentration. The mean concentration almost monotonically decreases with height except for in the immediate vicinity of the tail pipes. In Case-A2, the mean concentration level within the passing area is higher than that of Case-A1 because vertical dispersion to the upper direction and horizontal dispersion to the upwind direction are suppressed when horizontal advection is dominant. Note that the all concentration values are non-dimensionalized with  $V_a$ , therefore the actual concentration of Case-A2 is lower than that of Case-A1. When traffic is two-way (Case-B1,B2), the same features of the one-way case can be seen for the mean concentration distribution.

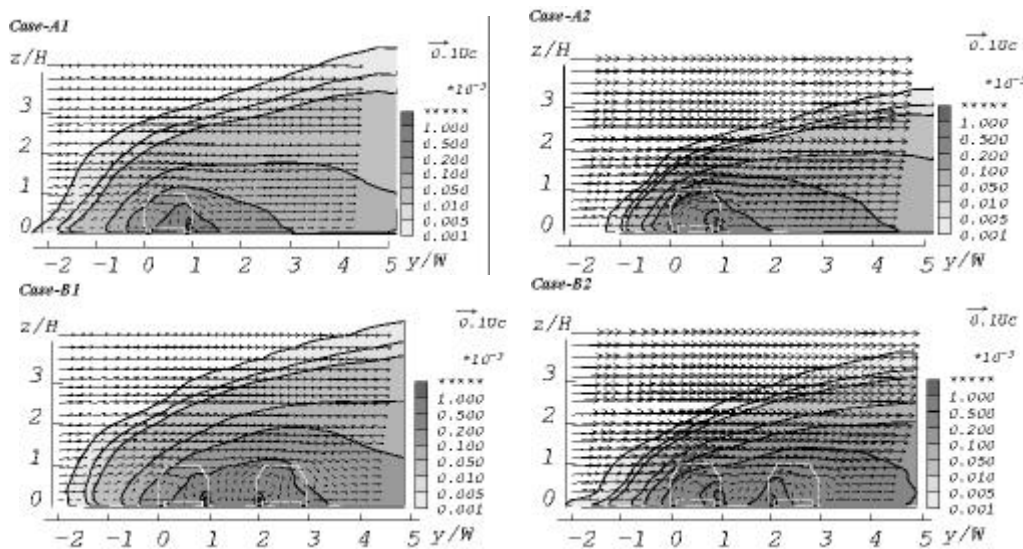


Fig.4; Time-space averaged velocity vectors and concentration distributions.

To compare our results with a Gaussian model, a vertical plume width was estimated from the mean concentration distribution on the y-z cross section by using the following equation:

$$s_z^2 = \int_0^\infty z^2 \langle C^* \rangle dz / \int_0^\infty \langle C^* \rangle dz \quad (1)$$

where  $s_z$  is the vertical plume width and  $\langle C^* \rangle$  is the time-space averaged non-dimensional concentration. Fig.5 shows spanwise variations of the  $s_z$  in Case-A1 and B1 ( $V_a=1.0 \text{ m s}^{-1}$ ) and in Case-A2 and B2 ( $V_a=2.0 \text{ m s}^{-1}$ ). Except in the vicinity of the tail pipe positions, the growth rate of the  $s_z$  about the downwind distance (in the y direction) are not so much different between one-way and two-way facing traffic cases. This means that, in the two-way traffic case, the vertical dispersion of the exhaust gas is mainly governed by the turbulence induced by the vehicles running on the upwind side lane. When a Gaussian line source model is used for a roadside air quality assessment, vertical plume width is often modified to account the influence of vehicle-induced turbulence, for example:

$$s_z = s_{z0} + s_{zp} \quad (2)$$

where  $s_{zp}$  is a vertical plume width given by Pasquill-Gifford chart, and  $s_{z0}$  is an initial dispersion width parameter. In Fig.5, the vertical plume width classified into category A (extremely unstable, PG-A) and D (neutral, PG-D) in Pasquill's stability are also plotted. Though the growth rate of  $s_z$  is larger than that of PG-A curve within the passing area, the  $s_z$  gradually approaches to the PG-D curve in the cross flow wake region. The  $s_{z0}$  estimated to fit the PG-D curve is  $1.25H$  for Case-A1,B1 and  $0.85H$  for Case-A2,B2, respectively. For  $s_{z0}$ , a fixed value comparable to the vehicle's height is often chosen, however, the  $s_{z0}$  value seems to depend on the cross flow velocity in our results.

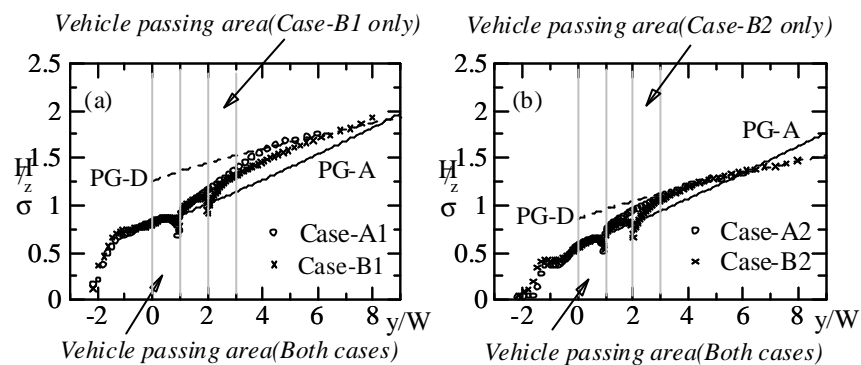


Fig.5; Spanwise profiles of the vertical plume width.  
(left;  $V_a=1.0 \text{ m s}^{-1}$ , right;  $V_a=2.0 \text{ m s}^{-1}$ , PG-A: stability A, PG-D: stability D)

## CONCLUSION

In this study, a numerical model based on LES concept was developed, and the distribution patterns of the time-space averaged flow and concentration on a one-way and a two-way road were estimated for sedan car passing cases.

- (1) The mean flow pattern is significantly different between the one-way and the two-way facing traffic cases, however, the magnitude of the mean flow is relatively small. On the other hand, the standard deviations of spanwise and vertical fluctuation velocities are two times larger than the maximum of the mean velocity in the vehicle passing area.
  - (2) The mean concentration monotonically decreases with height except for in the immediate vicinity of the tail pipes, so a ground level source approximation is justified.
  - (3) The growth rate of the vertical plume width in the cross flow wake region is not so much different between the one-way and the two-way traffic cases, and the rate is almost agreed with that of the category D curve in Pasquill's stability.
  - (4) The dependence of the initial dispersion width on the cross flow velocity is suggested.
- The modelling of vehicle-induced turbulence and its effect on the turbulent dispersion of pollutants for RANS simulation is our future work.

## ACKNOWLEDGEMENTS

This research was partially supported by Japan Society for the Promotion of Science (JSPS), Grant-in-Aid for Scientific Research(C), 18510025, 2006.

## REFERENCES

- Walcek, C.J., 2002: Minor flux adjustment near mixing ratio extremes for simplified yet highly accurate monotonic calculation of tracer advection, *J. Geophys. Res.*, **105**, D7, 9335-9348
- Werner, H. and H. Wengle, 1991: Large eddy simulation of turbulent flow over and around a cube in a plate channel, *Turbulent Shear Flows* 8, 155-168, Springer-Verlag, Germany